Available online at www.sciencedirect.com

Journal of the European Ceramic Society 24 (2004) 1141–1144

www.elsevier.com/locate/jeurceramsoc

# High resolution neutron powder diffraction study of the microstrain contribution in $Pb(Zr_xTi_{1-x})O_3$ ceramics

J. Frantti[a,*], S. Eriksson[b], S. Hull[c], S. Ivanov[d], V. Lantto[e], J. Lappalainen[e],
M. Kakihana[a]

[a]Tokyo Institute of Technology, Materials and Structures Laboratory, 4259 Nagatsuta, Midori-ku, Yokohama 226-8503, Japan
[b]Studsvik Neutron Research Laboratory, Uppsala University, SE-611 82, Nyköping, Sweden
[c]The ISIS facility, Rutherford Appleton Laboratory, Chilton, Didcot, Oxfordshire OX11 0QX, UK
[d]X-Ray Laboratory, Department of Inorganic Materials, Karpov Institute of Physical Chemistry, RU-103064 K-64, Moscow, Russia
[e]University of Oulu, Microelectronics and Materials Physics Laboratories, PO Box 90014 University of Oulu, Finland

## Abstract

The high-resolution neutron powder diffraction data collected from $Pb(Zr_xTi_{1-x})O_3$ ($x=0.20$, 0.52, 0.53 and 0.54) samples between 4 and 900 K were analysed using Rietveld refinement. The high-resolution powder diffractometer (HRPD) at Rutherford Appleton Laboratory (ISIS facility) was used. Particular attention was paid to two phase coexistence in the vicinity of the morphotropic phase boundary and to the microstrain contribution. Strongly reflection indices (*h*,*k*,*l*) dependent line broadening was related to a spatial variation of *x* which probes the sensitivity of different crystal lattice spacings against *x*.

© 2003 Elsevier Ltd. All rights reserved.

*Keywords:* Microstructure-final; PZT

*PACS:* 77.84.Dy; 61.12.Ld; 61.50.Ah; 81.30.Dz

## 1. Introduction

Despite the 50 year old history of lead zirconate titanate [$Pb(Zr_xTi_{1-x})O_3$ (PZT)] ceramics its structural details are still not well known and correspondingly there is no model which can quantitatively explain the high values of piezoelectric constants and electromechanical coupling coefficients. Recently, Noheda et al.[1] discovered a monoclinic *Cm* phase for compositions with $x=0.52$. Correspondingly, there have been attempts to model the piezoelectrical properties of single phase *Cm* crystals.[2] Our motivation for this study was to clarify the structural details of $x=0.20,0.52,0.53$ and $x=0.54$ samples [the latter three samples corresponding to the compositions in the vicinity of the morphotropic phase boundary (MPB)]. Although PZT ceramics with $x=0.20$ should be tetragonal below 440 °C,[3] there was a need to confirm that there is no average deviation from the *P*4*mm* symmetry. This is a starting point prior to the lattice dynamical computations. Raman scattering has revealed peak splitting, which was not consistent with the space group *P*4*mm* (for a discussion, see Ref. 4).

In a case of $x\approx0.52$ samples there have been several recent reports assigning different space groups at the same temperature for samples with nominally the same composition. Further, there has even been ambiguity concerning their single phase nature. To clarify this situation we collected high-resolution neutron powder diffraction data at several temperatures from the $x=0.54$ sample. Both the high resolution and neutrons are crucial once the space group symmetries are determined.

It was found that the apparently contradictory results can be neatly explained once one assumes that the Zr/Ti ratio is generally not the same among different crystals in PZT ceramics.[4] It is crucial to have a physically meaningful description for the "microstrain" as it affects the determination of structural parameters. In this article, we describe the modelling of the microstrain and discuss the connection between the refined profile

---

[*] Corresponding author.

0955-2219/$ - see front matter © 2003 Elsevier Ltd. All rights reserved.
doi:10.1016/S0955-2219(03)00582-X

parameters and microstrain. Structural parameters will be published later.

## 2. Experimental

PZT samples were prepared through conventional solid state reaction techniques. First, oxides were mixed and ball milled in a desired composition ratio, pellets were pressed, annealed at Pb-rich atmosphere at 800 °C, ground and ball milled and sintered at 1100 °C. Finally, surface layers were removed and pellets were ground into powder form. The compositions values referred to in this study are nominal compositions, which correspond to average composition.[4] The *average* Zr/Ti ratio is accurately controlled by the solid state reaction technique, and the slight Pb loss (due to the volatile PbO) occurring during the sintering can be compensated for by using Pb rich atmosphere and by removing the surface layers.

Neutron powder diffraction (NPD) data were collected at the Rutherford Appleton laboratory (ISIS facility) using the high-resolution powder diffractometer (HRPD). For NPD measurements PZT powders were put into a vanadium can. Helium cryostat and furnace were used for the low and high temperature measurements, respectively. As the resolution of this instrument is high, it reveals the line broadening essentially due to the sample itself. For Rietveld refinements, we used the GSAS software.[5] The line shape used in a case of $x=0.52$, 0.53 and 0.54 samples was the one by Stephens'[6] (GSAS line shape 4) and takes the microstrain contribution phenomenologically into account. Data collected at bank 1 (backscattering bank, which corresponds to the highest resolution data) were used. Our attention was paid to *hkl*-dependent line broadening and correct space group determination.

## 3. Results and discussion

The high temperature structure of all PZT ceramics is cubic (space group *Pm*3*m*). The low temperature NPD pattern of the $x=0.20$ sample was consistent with the *P*4*mm* symmetry. The other samples were modelled using two coexisting phases, monoclinic *Cm* and rhombohedral *R*3*c*. In a case of the $x=0.54$ sample, we still used the *Cm* and *R*3*c* symmetries to model the symmetries at 583 K, although the structural parameters of the *Cm* and *R*3*c* phases nearly corresponded to *P*4*mm* and *R*3*m* symmetries, respectively. During the refinement of the rhombohedral phase, *R*3*c* symmetry was used and the oxygen $y$ coordinate was constrained to be twice that of the $x$ coordinate. We did not find evidence for the space group *Cc* (subgroup of the space group *R*3*c*) and, as previously, we used the highest symmetry consistent with the diffraction pattern.[4]

### 3.1. Microstrain contribution

The GSAS line shape 4 assumes that each crystallite has its own lattice parameters, and parameters $S_{HKL}$ reflect the anisotropic line broadening. Origin of the microstrain in our case is dominantly due to the composition fluctuation, although there are probably many contributions to the microstrain, e.g., due to dislocations. It is worth noting that instrumental resolution might not always be sufficient to reveal this type of line broadening (unless some of the Bragg reflections are clearly depressed in intensity). The whole pattern fitting approach is crucial for PZT ceramics with compositions close to MPB, as there are two coexisting symmetries and, with only a few exceptions, the Bragg reflections from different phases overlap. Thus, it would be hopeless to do a Williamson–Hall plot for the PZT ceramics (except at sufficiently high temperatures where the two symmetries have transformed to the cubic symmetry, see an example in Ref. 7). For the same reason it is difficult to extract accurate crystal size distribution from the diffraction data: each mechanism affecting on the diffraction line width has to be correctly modelled. In the case of PZT and large grain size (say, ceramics prepared through the solid state reaction technique) the grain size distribution is easier to estimate using the scanning electron microscope. In the case of powders obtained by grinding the ceramics pellets it is more relevant to refer to a crystal size distribution, instead of the grain size distribution. We feel that in this type of situation Rietveld refinement offers the most reliable way of determining the *hkl*-dependent line broadening, as the same set of parameters is used to describe all reflections. One has to know (based on an assumed structure) exactly the number of reflections and their intensities at each region. Correspondingly, we decided to use the whole-pattern-fitting approach, instead of limiting our study to just some selected peaks.

After refining the $S_{HKL}$ parameters, we estimated the microstrain SS using the equation

$$S_S(hkl) = d_{hkl}^2 \sqrt{\sum_{HKL} S_{HKL} h^H k^K l^L}$$

(Ref. 5, p. 157) where $H+K+L=4$, $d_{hkl}$ is the distance between lattice planes and C is the diffractometer constant (approximately 48235 μs Å$^{-1}$). Parameters $S_{HKL}$ are constrained to fulfil the symmetry of the crystal system and are given in Refs. 5 and 6. To visualise these parameters, we plotted $S_S(hkl)$ as a function of two indices (such as $h$ and $k$) and kept the third (now $l$) as constant. Fig. 1 shows the microstrain for $x=0.54$

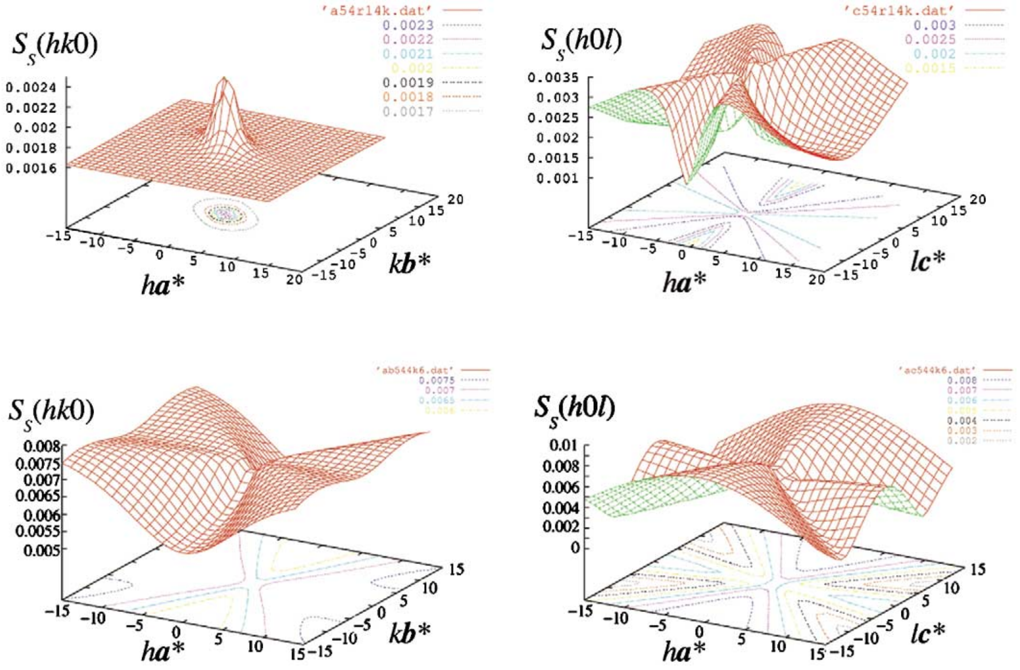

Fig. 1. Microstrain of the $x=0.54$ sample in the case of the rhombohedral $R3c$ phases (up) and monoclinic $Cm$ (below) on two reciprocal lattice planes at 4 K. Note the scale difference between the upper and lower graphs.

sample in different reciprocal planes for $Cm$ and $R3c$ symmetries.

$S_S(hkl)$ contains useful information about "soft" crystal directions (which may not be the crystal axes directions) against composition variation (which are often different to their variation with temperature). In the case of $Cm$ and $R3c$ symmetries, comparison between the anisotropic strain $\Delta d/d = S_S$ and experimental NPD data is possible only for indices obeying the conditions $h+k=2n$ ($Cm$ symmetry) and $-h+k+l=3n$ ($R3c$ symmetry and hexagonal observe setting), where $n$ is any integer.

Fig. 1 shows that the microstrain was significantly larger in the case of the $Cm$ phase than in the case of the $R3c$ phase. Further, microstrain decreases with increasing temperature. Topolev and Turik[8] concluded that the monoclinic phase relieves the stress, which would otherwise be generated due to the interacting rhombohedral and tetragonal phases in the vicinity of MPB.

## 4. Conclusions

Space group symmetries and microstrain contribution to the diffraction profiles of PZT samples with $x=0.20, 0.52, 0.53$ and 0.54 were studied by high-resolution neutron powder diffraction. The case of an $x=0.20$ sample, the only symmetries observed were $P4mm$ (low temperature symmetry) and $Pm3m$ (high temperature symmetry). Thus, one has to look for another explanation than average symmetry lowering for the observed Raman peak splitting. Samples having composition in the vicinity of the morphotropic phase boundary had two different phase symmetries (except at high temperature). To explain the observed neutron powder diffraction profiles, we assumed that Zr/Ti ratio is not constant among different crystallites. Spatially varying Zr/Ti ratio explains the following features: (i) two phase "coexistence" and the dependence of the phase fractions on composition and temperature in the vicinity of the MPB, (ii) anomalous line shape of the diffraction profiles. The fact that the microstrain in the rhombohedral phase was small gave support to the previously presented ideas that the $Cm$ phase is a consequence of interacting tetragonal and rhombohedral phases. This further suggests that the area of the $Cm$ phase in $x$-$T$ plane is sensitive to the variation in composition and to other imperfections.

## Acknowledgements

We are grateful to Dr. Robert Von Dreele for his useful suggestions concerning the refinement procedure. One of us (J.F.) is thankful to the Vilho, Yrjö ja Kalle Väisälä foundation and the Japan Society for the Promotion of Sciences (Contract No. 13001738) for the financial support.

## References

1. Noheda, B., Cox, D. E., Shirane, G., Gonzalo, J. A., Cross, L. E. and Park, S.-E., *Appl. Phys. Lett.*, 1999, **74**, 2059.
2. Bellaiche, L., Garcia, A. and Vanderbilt, D., *Phys. Rev. Lett.*, 2000, **84**, 5427.
3. Jaffe, B., Cook, W. R. and Jaffe, H., *Piezoelectric Ceramics.* Academic Press, London, 1971.
4. Frantti, J., Ivanov, S., Eriksson, S., Rundlöf, H. V., Lantto, J., Lappalainen, H. and Kakihana, M., *Phys. Rev.*, 2002, **B66**, 064108.
5. Larson, A. C. and Von Dreele, R. B., General structure analysis system (LANSCE, MS-H805, Los Alamos National Laboratory, Los Alamos, NM 87545) 2000.
6. Stephens, P. W., *J. Appl. Cryst.*, 1999, **32**, 281.
7. Noheda, B., Gonzalo, J. A., Cross, L. E., Guo, R., Park, S.-E., Cox, D. E. and Shirane, G., *Phys. Rev.*, 2000, **B61**, 8687.
8. Topolev, Yu. and Turik, A. V., *J. Phys.: Condens. Matter*, 2001, **13**, L771.